

The dynamic mechanical behaviour of carbon black filled EPDM parallel and series models

John Luthern

Mount Union College, Alliance, OH 44601-3993, USA
(Received 4 June 1991; revised 30 November 1992)

The mechanical, elastic and viscoelastic properties of an elastomer are affected by the addition of carbon black. Incorporation of carbon black into an elastomeric matrix increases tensile strength, the complex dynamic modulus and hysteresis among other properties. Dynamic mechanical properties of elastomers filled with polymeric and non-polymeric fillers can be described in terms of certain mechanical models proposed by Takayanagi. In the case of a two-component series model, equations have been developed to predict the individual strain in each phase when testing under position control. Utilizing the loss modulus and the square of the dynamic strain amplitude of each phase, it is possible to calculate the hysteresis in each section. Based on the assumption that the model hysteresis is a weighted average of individual hysteretic contributions, the energy loss per cycle of the series model may be predicted. This approach is also utilized in the case of a two-component parallel model.

(Keywords: EPDM; carbon black; dynamic mechanical behaviour)

INTRODUCTION

Mechanical models have frequently been utilized to facilitate the calculation of the viscoelastic properties of heterogeneous polymer systems¹. In the early 1960s Takayanagi² utilized simple mechanical models to calculate the viscoelastic behaviour of a variety of multicomponent systems. The basis of the model is a parallel arrangement consisting of both crystalline and amorphous regions, each with their own set of viscoelastic properties. When the two regions are in parallel the dynamic modulus may be calculated via the Voigt averaging scheme:

$$E^* = \lambda E_A^* + (1 - \lambda) E_C^* \quad (1)$$

where λ is the volume fraction of the amorphous phase perpendicular to the direction of the applied force, $(1 - \lambda)$ is the volume fraction of the crystalline phase perpendicular to the direction of the applied force, and the subscripts A and C refer to the amorphous and crystalline regions, respectively. When the two regions are connected in series the dynamic modulus may be calculated according to the Reuss averaging scheme:

$$\frac{1}{E^*} = \left(\frac{\psi}{E_A^*} + \frac{1 - \psi}{E_C^*} \right)^{-1} \quad (2)$$

where ψ is the volume fraction of the amorphous phase parallel to the direction of the applied force and $1 - \psi$ is the volume fraction of the crystalline phase parallel to the direction of the applied force.

Takayanagi² successfully predicted the storage and loss moduli and the loss tangent of a two-phase system composed of bonded poly(vinyl chloride) and styrene-butadiene rubber blocks utilizing equations (1) and (2) simultaneously. Prevorsek and Butler³ derived equations to predict E' (storage modulus), E'' (loss modulus), and $\tan \delta$ for crystalline nylon-6.

This study will attempt to account for the dynamic behaviour of a filled rubbery polymer in terms of the response of components representing carbon black filled and unfilled EPDM regions. The dynamic mechanical behaviour of a system consisting of series and parallel combinations of this type is of interest for at least two reasons: (1) to demonstrate the applicability of the Takayanagi models to a carbon black/EPDM system and (2) to suggest a potential method for the customization of the damping coefficient of commercial products based on the models and subsequent equations derived herein.

EXPERIMENTAL

Model preparation

The material utilized in this study was EPDM 2504 (Exxon). The filler employed was carbon black N550 supplied by the Continex Carbon Company. The curing agent was dicumyl peroxide-R (DICUP-R) supplied by Aldrich.

Master-batches containing 10, 25, 40, 55, 75 and 100 phr (i.e. parts per hundred parts rubber) carbon black were mixed on a small Banbury for a short time, dumped, and allowed to cool to ambient temperature. The master-batches were each allowed to band on the two-roll mill and 1.5 phr of DICUP-R was added to each batch, including a batch of unfilled EPDM that was similarly premasticated in the Banbury. The batches were then compression moulded into 2.5 cm \times 8.9 cm \times 0.2 cm rectangles and partially cured at 145°C for 30 min at which time the samples were removed from the press and cooled with tap water. The samples were punched out of the mould and cut into the desired shapes, then reinserted into the original rectangular mould in either series or parallel fashion. The samples were put back into the press

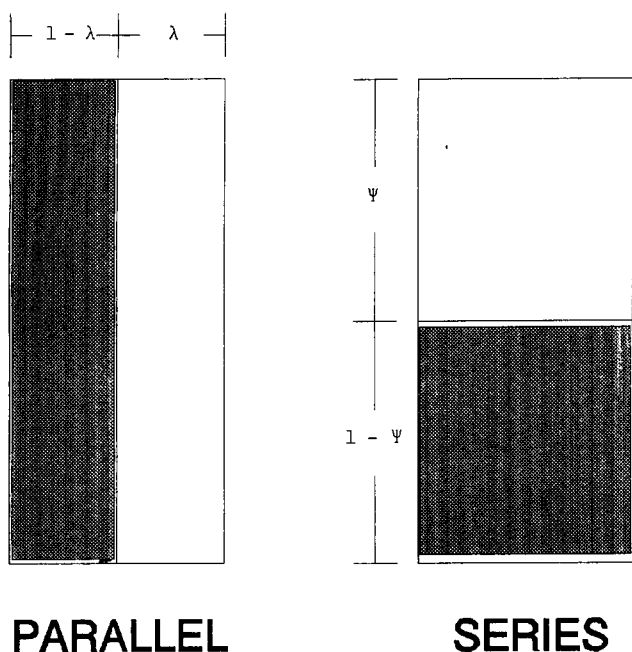


Figure 1 Illustration of series and parallel models

and cure was completed at 145°C. A representative diagram of both series and parallel models is provided in Figure 1.

Dynamic mechanical analysis

All dynamic characterizations were carried out on a servo-hydraulic, forced vibrational analyser made by CGS Instruments. All measurements were made at 25°C, at a frequency of 0.25 Hz, and at a small (<10%) and constant dynamic strain amplitude. The results were printed out on an X-Y plotter in the form of a Lissajou ellipse.

RESULTS AND DISCUSSION

Parallel model

For a parallel model consisting of two separate phases, the complex modulus is given by equation (1). Application of this equation to a parallel model, consisting of a carbon black filled EPDM phase (corresponding to the crystalline phase of Takayanagi's models) and an unfilled EPDM phase (corresponding to the amorphous phase of Takayanagi's model) with the filled phase loaded so as to maintain a constant overall carbon black loading, met with great success. Initially two sets of parallel models were constructed and dynamically characterized: set A, which contained three parallel models with an overall carbon black loading of 10 phr, and set B, which contained four parallel models with an overall carbon black loading of 25 phr. Figure 2 is a plot of the volume fraction of the unfilled phase perpendicular to the direction of the applied stress versus the dynamic complex modulus for set A models. Predicted and experimental values of E^* are within 5% of each other. Figure 3 is a plot of the volume fraction of the unfilled phase perpendicular to the direction of the applied stress versus the dynamic complex modulus for set B models. Predicted and experimental values are within 7% of one another which appears to validate the application of the Voigt

averaging scheme to a parallel system consisting of filled and unfilled EPDM phases.

In both sets A and B the overall hysteresis is simply the weighted average of the hysteresis of the individual components where the weight factors are the volume fractions of the individual components perpendicular to the direction of the applied stress (this was initially based on previous calculations and has since been proved experimentally):

$$W_s = \lambda(W_a) + (1 - \lambda)(W_c) \tag{3}$$

where W_s , W_a and W_c are the hysteresis of the system (i.e. model), unfilled phase and filled phase, respectively. λ is the volume fraction of the A component (the unfilled EPDM) perpendicular to the direction of the applied force and $(1 - \lambda)$ is the volume fraction of the C component (the carbon black filled EPDM) perpendicular to the direction of the applied force.

Based on the area of a dynamic stress-strain curve, the energy loss per cycle per unit volume is given by:

$$W_s = \frac{\pi}{4} (\epsilon_{dyn}^2) E''_s \tag{4}$$

where W_s , ϵ_{dyn} and E''_s are the system hysteresis, dynamic strain amplitude and loss modulus, respectively. Equation (4) holds true for any system analysed in this study, be it heterogeneous model or isolated A or

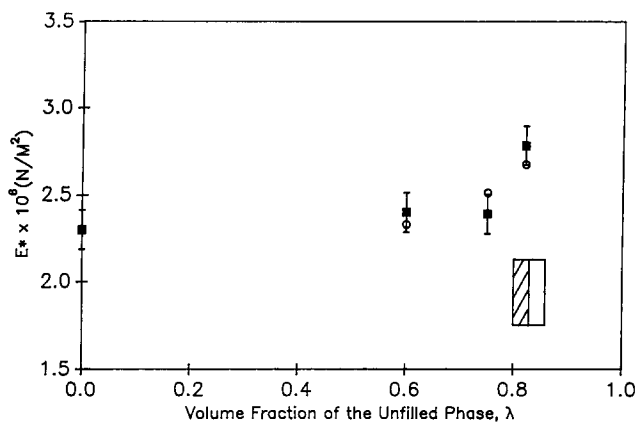


Figure 2 Dynamic modulus, E^* , versus the volume fraction of the unfilled phase for various parallel models at an overall carbon black loading of 10 phr. ■, Experimental; ○, theory, $E_s = \lambda E_A + (1 - \lambda) E_C$

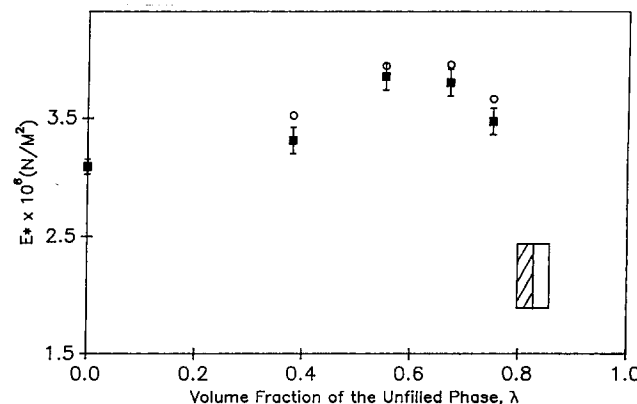


Figure 3 Dynamic modulus, E^* , versus the volume fraction of the unfilled phase for various parallel models at an overall carbon black loading of 25 phr. ○, Experimental; ■, theory, $E_s = \lambda E_A + (1 - \lambda) E_C$

C component. Subsequent to the determination of the viscoelastic behaviour of the isolated A and C components, the relative amounts of the A and C phases in the system may be adjusted to give any value of W_s in between those of the isolated A and C phases. By substituting equation (4) into equation (3), one obtains an equation predicting the hysteresis of the parallel model which yields, after rearrangement:

$$W_s = \frac{\pi}{4} \epsilon_{dyn}^2 [\lambda E_A'' + (1 - \lambda) E_C''] \quad (5)$$

where E_A'' is the loss modulus of the A phase and E_C'' is the loss modulus of the C phase.

Figure 4 is a plot of the volume fraction of the unfilled phase perpendicular to the direction of the applied stress versus the energy loss per cycle per unit volume for set A. The agreement between predicted and experimental values is good. Figure 5 is a plot of the volume fraction of the unfilled phase perpendicular to the direction of the applied stress versus the energy loss per cycle per unit volume for set B. There is qualitative agreement between predicted and experimental values which appears to validate the extension of the Voigt model and the applicability of equation (5) to this particular system.

The loss tangent gives an indication of how well a sample dissipates energy upon deformation in relation

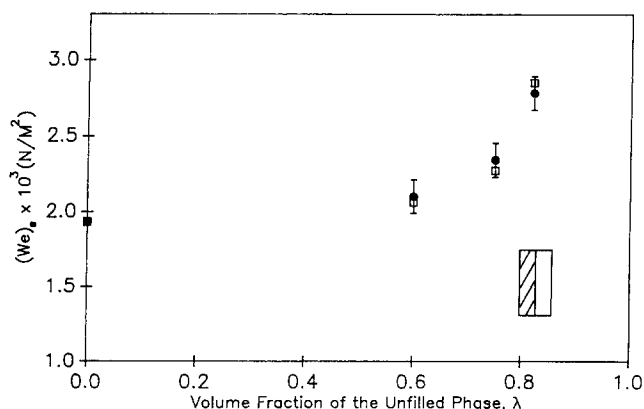


Figure 4 Energy loss per cycle per unit volume versus the volume fraction of the unfilled phase for various parallel models at an overall carbon black loading of 10 phr. ●, Experimental; □, theory, $(W_e)_s = (\pi/4)\epsilon[\lambda E_A'' + (1 - \lambda)E_C'']$

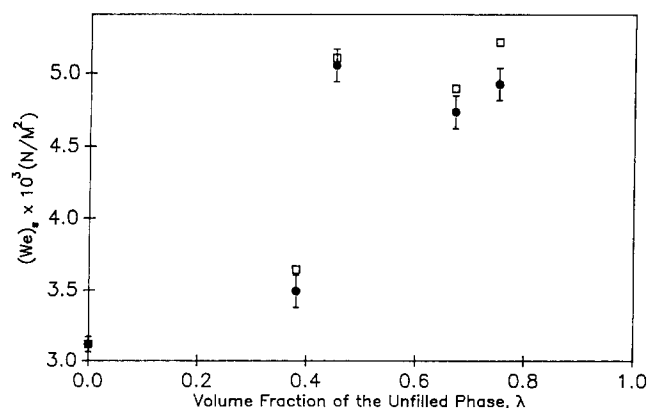


Figure 5 Energy loss per cycle per unit volume versus the volume fraction of the unfilled phase for various parallel models at an overall carbon black loading of 25 phr. ●, Experimental; □, theory, $(W_e)_s = (\pi/4)\epsilon[\lambda E_A'' + (1 - \lambda)E_C'']$

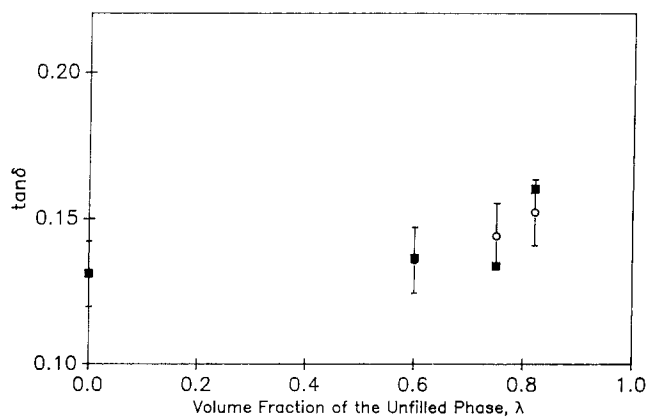


Figure 6 Loss tangent versus volume fraction of the unfilled phase for various parallel models at an overall carbon black loading of 10 phr. ○, Experimental; ■, theory, $\tan \delta_s = [\lambda \sin \delta_A + (1 - \lambda)X_C \sin \delta_C] / [\lambda + (1 - \lambda)X_C]$

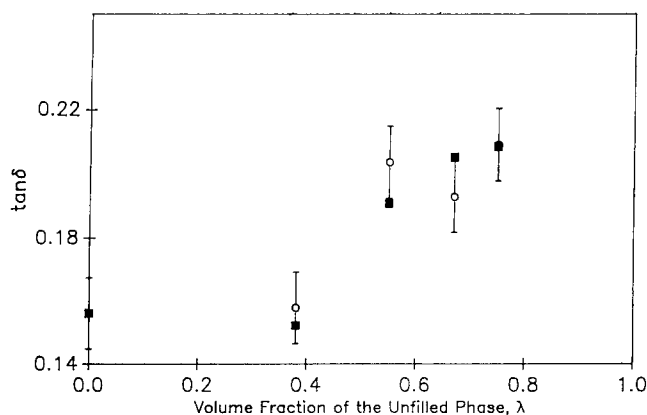


Figure 7 Loss tangent versus volume fraction of the unfilled phase for various parallel models at an overall carbon black loading of 25 phr. ○, Experimental; ■, theory, $\tan \delta_s = [\lambda \sin \delta_A + (1 - \lambda)X_C \sin \delta_C] / [\lambda + (1 - \lambda)X_C]$

to how well the sample will store energy elastically. For a simple parallel model $\tan \delta_s$ is given by the following:

$$\tan \delta_s = \frac{\lambda \sin \delta_A + (1 - \lambda)X_C \sin \delta_C}{\lambda + (1 - \lambda)X_C} \quad (6)$$

where $\tan \delta_s$ is the loss tangent of the system, $\sin \delta_A$ and $\sin \delta_C$ are the sines of the phase angle, δ , of components A and C respectively, and X_C is the strain amplification factor of the filled phase due to the presence of carbon black⁵⁻⁷. For purposes of calculations X_C was determined experimentally from the isolated components via the following relation:

$$E_C = E_A X_C \quad (7)$$

where E_A and E_C are the moduli of the unfilled and filled components, respectively. Figures 6 and 7 are plots of experimental and predicted $\tan \delta$ values for sets A and B, respectively. There is good qualitative agreement between experimental values and those predicted by equation (6), which implies that the $\tan \delta$ of the model depends upon the weighted $\sin \delta$ values of both A and C phase, the weight factors determined by the volume fractions of the A and C phase perpendicular to the direction of the applied stress and the strain amplification factor of the filled C phase.

Series model

For a model consisting of two components connected in series, the stresses of each component are equal and are also equal to the overall stress experienced by the model. The overall strain is a sum of the individual strains found in each component. The complex modulus of a simple series model is given by the Reuss average (equation (2)) where in this case the subscript A refers to the unfilled phase and the subscript C refers to the filled phase.

The first set of series models constructed consisted of one carbon black filled EPDM phase and an unfilled EPDM phase with the correct concentration of carbon black in the filled phase to give an approximate overall filler loading of 25 phr. These models will be referred to as set C. Utilizing equation (2) to predict the viscoelastic behaviour of set C, the calculated and experimental values of set C are plotted versus the volume fraction of the unfilled phase parallel to the direction of the applied stress in Figure 8. The predicted and experimental values fell within 10% of one another, which implies that equation (2) is satisfactory when applied to the system in question. Based on the fact that

$$\epsilon_s = \psi \epsilon_A + (1 - \psi) \epsilon_C \tag{8}$$

where ϵ_A is the dynamic strain amplitude of the A phase, ϵ_s is the total dynamic strain amplitude and ϵ_C is the dynamic strain amplitude of the C phase, it may be shown that

$$\epsilon_A = \epsilon_s \left[\frac{(1 - \psi)}{K} + \psi \right] \tag{9}$$

where $K = E_C/E_A$ and

$$\epsilon_C = \epsilon_s - \frac{\epsilon_A \psi}{1 - \psi} \tag{10}$$

The energy loss per cycle occurring in the A phase is given by:

$$(W_A)_s = \frac{\pi}{4} \left\{ \frac{\epsilon_s}{\left[\frac{(1 - \psi)}{K} + \psi \right]} \right\}^2 E''_A \tag{11}$$

where $(W_A)_s$ is the energy loss per cycle per unit volume occurring in the A phase and E''_A is the loss modulus of the A phase. The hysteresis occurring in the C phase is

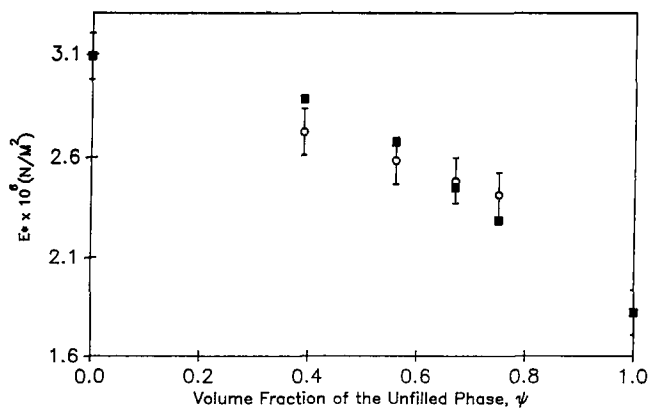


Figure 8 Dynamic modulus, E^* , versus volume fraction of the unfilled phase for various series models at an overall carbon black loading of 25 phr. \circ , Experimental; \blacksquare , theory, $E^* = [\psi/E_A + (1 - \psi)/E_C]$

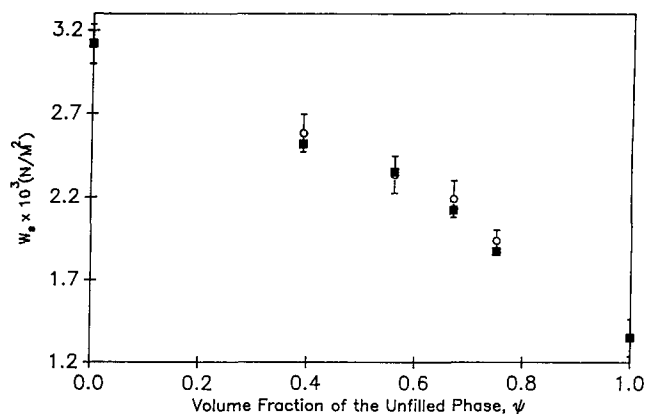


Figure 9 Energy loss per cycle per unit volume versus volume fraction of the unfilled phase for various series models at an overall carbon black loading of 25 phr. \circ , Experimental; \blacksquare , theory, $W_s = \psi(W_A) + (1 - \psi)(W_C)$

given by:

$$(W_C)_s = \frac{\pi}{4} \left(\frac{\epsilon_s - \epsilon_A \psi}{1 - \psi} \right)^2 E''_C \tag{12}$$

where $(W_C)_s$ is the hysteresis occurring in the C phase and E''_C is the loss modulus of the C phase.

Similarly to the parallel model, the hysteresis of the series model is the weighted sum of the hysteresis of the components and is given by:

$$W_s = \psi(W_A)_s + (1 - \psi)(W_C)_s \tag{13}$$

Figure 9 is a plot of the energy loss per cycle per unit volume versus the volume fraction of the unfilled phase parallel to the direction of the applied stress. There is excellent agreement between predicted and experimental values, which implies that the system hysteresis is dependent upon $\sin \delta_A$, $\sin \delta_C$, E''_A , E''_C and ϵ_s and equation (13) is valid for at least the carbon black filled/unfilled EPDM model of this study.

The loss tangent of the series model is given by:

$$\tan \delta_s = \frac{1}{\alpha^2} \left[\frac{\psi \tan \delta_A}{X_s} + \left(\frac{\alpha^2}{1 - \psi} - 2\psi\alpha + \psi^2 \right) v \tan \delta_C \right] \tag{14}$$

where $\alpha = [(1 - \psi)/K + \psi]$, $v = X_C/X_s$, $X_C = E_C/E_A$ and $X_s = (\psi + 1 - \psi/X_C)^{-1}$. The experimental and predicted values of $\tan \delta$ are within 13% of one another for set C and are plotted versus ψ in Figure 10.

Parallel models consisting of two phases filled with variable carbon black loadings

Thirteen parallel models consisting of two components containing 0, 10, 25, 40 or 55 phr carbon black, hereafter referred to as set D, were constructed and subjected to dynamic characterization. Dynamic testing was carried out at a small and constant dynamic strain amplitude, at 25°C and at a frequency of 0.25 Hz. The isolated components were also tested dynamically under identical conditions. Figure 11 is a plot of each model's dynamic modulus versus carbon black loading for set D. Predicted results were obtained by utilizing equation (1) and the viscoelastic data from the dynamic analysis of each individual phase, i.e. the 0, 10, 25, 40 and 55 phr carbon black EPDM batches. There is excellent agreement

between predicted and experimental results with slight deviation from theory at carbon black loadings above 45 phr. This indicates that a predetermined $\tan \delta$ value may be attained with a high degree of accuracy if that $\tan \delta$ value lies between the $\tan \delta$ values of the two individual components used to construct the model.

Figure 12 is a plot of the energy loss per cycle per unit volume versus carbon black loading for the variably loaded carbon black parallel models. Utilizing dynamic

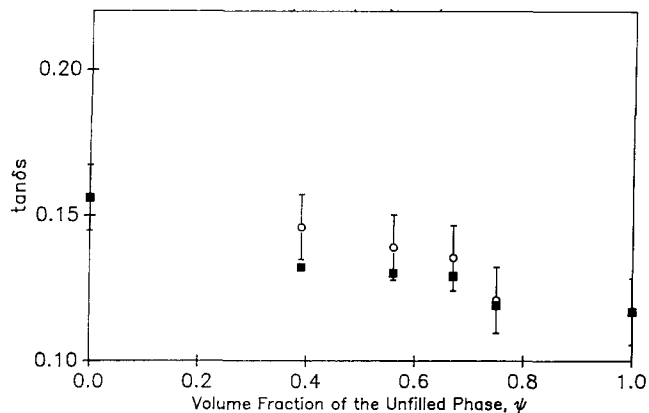


Figure 10 Loss tangent versus volume fraction of the unfilled phase for various series models at an overall carbon black loading of 25 phr. \circ , Experimental; \blacksquare , theory, $\tan \delta_s = (\psi \tan \delta_A / X_s) + (\alpha^2 - 2\psi\alpha + \psi^2)(1/1 - \psi) \tan \delta_c (1/\alpha^2)$

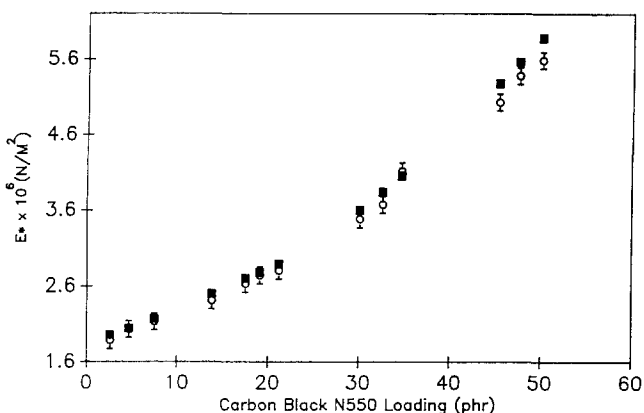


Figure 11 Dynamic modulus, E^* , versus carbon black loading for various parallel models. \circ , Experimental; \blacksquare , theory, $E^* = \lambda E_A + (1 - \lambda) E_C$

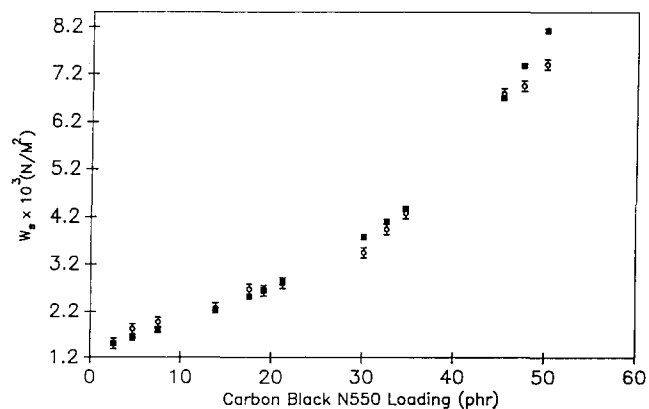


Figure 12 Energy loss per cycle per unit volume versus carbon black loading for various parallel models. \circ , Experimental; \blacksquare , theory, $W_s = \lambda(W_A) + (1 - \lambda)(W_C)$

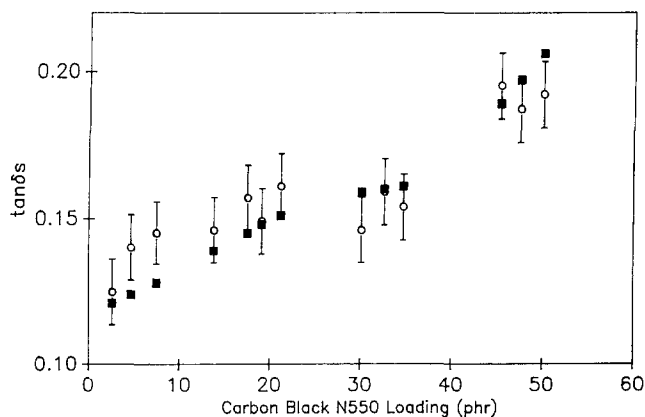


Figure 13 Loss tangent versus carbon black loading for various parallel models. \circ , Experimental; \blacksquare , theory, $\tan \delta_s = [\lambda(\sin \delta_A)(X_A) + (1 - \lambda)(X_C)(\sin \delta_C)] / [\lambda(X_A) + (1 - \lambda)(X_C)]$

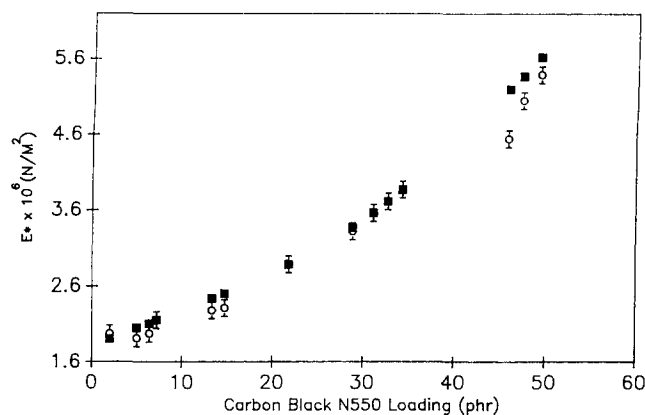


Figure 14 Dynamic modulus, E^* , versus carbon black loading for various series models. \circ , Experimental; \blacksquare , theory, $1/E^* = (\lambda/E_A^* + (1 - \lambda)/E_C^*)^{-1}$

data from the analysis of the individual components and equation (5), predicted and experimental hysteresis values were within 10%. $\tan \delta$ values were calculated according to equation (6) when one component of the parallel model was unfilled EPDM; however, in cases when each of the two components contained carbon black, equation (6) was rearranged to yield:

$$\tan \delta_s = \frac{\lambda \sin \delta_A + (1 - \lambda) X_C \sin \delta_C}{\lambda X_A + (1 - \lambda) X_C} \quad (15)$$

where X_A is the strain amplification factor of the phase with the smaller degree of carbon black loading. Figure 13 is a plot of $\tan \delta_s$ for the set D models. The predicted results obtained from equation (15) and experimental values showed reasonable agreement, i.e. within 15%.

Series models containing two phases filled with variable carbon black loadings

Fifteen series models containing two phases filled with any of the loadings 0, 10, 25, 40 and 55 phr carbon black, referred to as set E, were subjected to dynamic characterization. The models were tested at a small and constant dynamic strain amplitude, at 25°C and at a frequency of 0.25 Hz. The isolated phases were also characterized dynamically under identical conditions. Figure 14 is a plot of the dynamic modulus versus overall carbon black loading for all set E models. Utilizing equation (2) for calculating modulus values, there is good

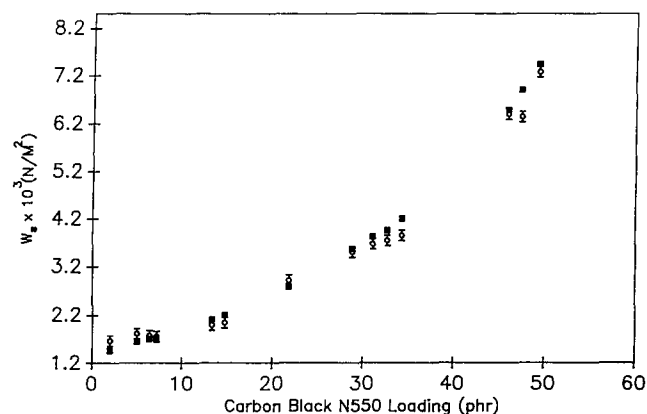


Figure 15 Energy loss per cycle per unit volume versus carbon black loading for various series models. ○, Experimental; ■, theory, $W_s = \psi(W_A) + (1 - \psi)(W_C)$

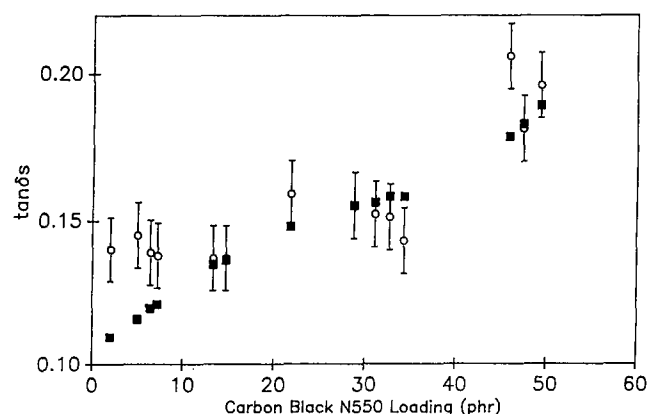


Figure 16 Loss tangent versus carbon black loading for various series models. ○, Experimental; ■, theory, $\tan \delta_s = (1/\alpha^2)\{\chi \sin \delta_A/X_s\} + [(\alpha^2/(1-\chi) - 2\chi\alpha + \chi^2)(X_C/X_s) \sin \delta_C]\}$

agreement between predicted and experimental results. Combining equations (9), (10), (11), (12) and (13), and after rearrangement, the following equation is obtained:

$$W_s = \frac{\pi}{4} \left\{ \psi \frac{\epsilon_s}{\alpha^2} E_A + \frac{E_C [\epsilon_s (1 - \psi)^2 - 2\epsilon_s^2 \psi \alpha (1 - \psi) + \psi^2 \epsilon_s \alpha^2]}{1 - \psi} \right\} \quad (16)$$

The predicted values for the hysteresis of set E are plotted along with experimental values versus the overall model carbon black loading in Figure 15. Again there is good agreement between predicted and experimental values, which indicates that system hysteresis depends upon the individual strain in each component which is related to the overall strain through the stiffness of each component; this is itself dependent upon the strain amplification present in each phase, the volume fraction of each component perpendicular to the direction of the applied stress and the loss modulus of each phase. Equation (14) was used to calculate $\tan \delta$ values for set E and the predicted and experimental values are plotted versus the overall carbon black loading in Figure 16. Good qualitative agreement indicates the validity of the equation; however, the slight deviations (<20%) at low carbon black loadings are not yet understood.

CONCLUSIONS

It appears to be possible to predict the viscoelastic behaviour of parallel and series models containing two EPDM phases of different carbon black loadings under position control using the following assumptions:

1. the modulus of the filled material will increase according to the strain amplification factor, X;
2. the energy loss per cycle per unit volume increases with the square of the strain amplification factor.

Equations have been proposed which were successful in calculating the hysteresis and loss tangent of simple parallel and series models and take into account the viscoelastic properties of each component.

REFERENCES

- 1 Dickie, R. A. *Polym. Sci.* 1973, **17**, 45
- 2 Takayanagi, M. *Am. Chem. Soc. Div. Org. Coatings, Plast. Chem., Prepr.* 1963, **23** (2), 75
- 3 Prevorsek, D. and Butler, R. H. *Int. J. Polym. Mater.* 1972, **1**, 251
- 4 Luthern, J. PhD dissertation, The University of Akron, 1991
- 5 Einstein, A. *Am. Phys. (Leipzig)* 1906, **19**, 289
- 6 Guth, E. and Gold, O. *Phys. Rev.* 1938, **53**, 322
- 7 Meinecke, E. A. and Taftaf, M. *Rubber Chem. Technol.* 1988, **61**, 534